CHEMISTRY OF MATERIALS

Article

pubs.acs.org/cm

Cyclodextrin/Paclitaxel Complex in Biodegradable Capsules for Breast Cancer Treatment

Jing Jing,[†,‡] Anna Szarpak-Jankowska,[†,‡] Raphael Guillot,[§] Isabelle Pignot-Paintrand,[§] Catherine Picart,[§] and Rachel Auzély-Velty*[,†,‡]

[†]Centre de Recherches sur les Macromolécules Végétales (CERMAV-CNRS), 38041 Grenoble, France

[‡]Joseph Fourier University, 38041 Grenoble, France

[§]Grenoble Institute of Technology and CNRS, LMGP, 38041 Grenoble, France

Supporting Information

ABSTRACT: A novel type of biocompatible hollow capsules that combine severable favorable features as a hydrophobic drug carrier, including host−guest complexation in the shell, the unique biological functions of hyaluronic acid (HA), and transport properties of the multilayer shell, was designed and prepared. These capsules were generated by layer-by-layer (LbL) deposition of HA modified with β-cyclodextrin (CD) molecules and poly(L-lysine) (PLL) on calcium carbonate particles. Simultaneously, paclitaxel (PTX) was loaded in the LbL wall via host−guest interaction. Under physiological conditions, the incorporated anticancer drug was slowly released, and the capsules remained stable. Because the PTX molecules are selectively complexed by CD in the shell, their release can be triggered by the addition of competitive cyclodextrin molecules in the external medium. By incubating the capsules with breast cancer cells (MDA-MB-231), it was found that the cells bound specifically to the capsules through the CD44 receptor of HA that is overexpressed on their surface. Finally, when breast cancer cells were incubated with the PTX-loaded capsules, their viability was found to strongly decrease. All together, these results highlight the potential for these HA−cyclodextrin-containing capsules in anticancer therapy.

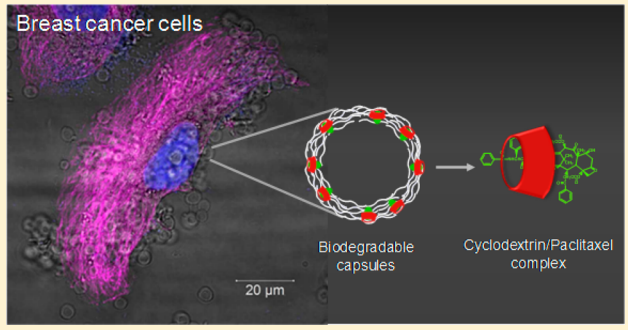

KEYWORDS: *layer-by-layer capsules, host−guest complexation, cyclodextrin, hyaluronic acid, drug release*

INTRODUCTION

The delivery of drugs is currently a great challenge in the field of nanobiotechnology, especially for hydrophobic compounds that constitute a great part of the currently available drugs.[1−3] Many of these compounds have been found to have limited clinical effectiveness partly because of their high toxicity, low solubility, and/or other poor pharmaceutical parameters. It has been demonstrated that conjugation of a poorly water-soluble molecule to a water-soluble polymer (called the prodrug approach) can greatly enhance its aqueous solubility and reduce its cytotoxicity in vitro and in vivo.[4] Nanoparticles are alternative materials that have shown huge potential for encapsulating and delivering poorly water-soluble compounds, especially in anticancer therapy.[5,6] These systems provide a more flexible approach compared to prodrugs, which are limited to hydrophobic drugs possessing a functionality for their chemical grafting on the polymer chain. However, even after decades of development, there are a few examples of nanotechnology-based therapeutic products that have been approved for clinical use.[5] One of the major obstacles is the initial burst release of the encapsulated drug, which increases the risk of toxicity. Moreover, most of the methods to produce polymeric nanoparticles involve the use of toxic solvents and surfactants that require intensive postprocessing purification.

Cyclodextrins (CDs) are water-soluble cyclic oligosaccharides that can include various guest molecules into their hydrophobic cavity, allowing the solubilization, stabilization, and transport of hydrophobic drugs.[7] Worldwide, 30−40 different drugs are now marketed as cyclodextrin complexes.[8] Although the use of CDs as solubilizers in the pharmaceutical field has been documented for decades, more advanced CD-based drug-delivery systems still need to be developed. In recent years, the nanoscale association of these host molecules with particles or polymers has led to the development of drug-delivery platforms with unique stimuli-responsiveness and adjustable drug-release characteristics. By immobilizing CD on magnetic nanoparticles, the ability to trigger the release of hydrophobic drugs incorporated in the CD through the use of induction heating was shown.[9] Using layer-by-layer (LbL) assembly of poly(carboxymethyl-β-cyclodextrin) complexed with a small molecule and positively charged degradable

Received: June 19, 2013
Revised: September 1, 2013
Published: September 4, 2013

poly(β-aminoesters), nanoscale coatings for small-molecule delivery capable of programmable release kinetics could be obtained.[2] These surface-eroding films were prepared under mild conditions.

The extension of this technology to LbL-based hollow capsules may offer new opportunities for designing carriers with tunable functionalities in the nano/micrometer range. These capsules, also called polyelectrolyte multilayer capsules, consist of two distinct compartments: the multilayer shell and the aqueous cavity. Such a structure may be advantageously used to achieve a bicompartment delivery for both hydrophobic and hydrophilic drugs with synergistic effects for the treatment of diseases such as cancer. In general, drugs are loaded into the aqueous cavity with a high loading efficiency. However, this implies that the drugs have good water-solubility and a relatively high molecular weight to avoid leakage from the capsules. Because many anticancer drugs, such as paclitaxel, doxorubicin, and camptothecin, are small hydrophobic molecules, it is still a challenge to load these drugs in the hydrophilic multilayer shell. Until now, few strategies have been reported for the incorporation of poorly water-soluble molecules in the capsule shell. Caruso et al. reported a prodrug approach in which the hydrophobic cancer drug paclitaxel (PTX) was covalently coupled to poly(L-glutamic acid) and embedded inside the capsule shell.[10] As an alternative strategy for the noncovalent sequestering of hydrophobic drugs, we developed hydrophobic nanoshells based on decylamino hydrazide derivatives of hyaluronic acid (HA).[11] However, this strategy, which is based on the nonspecific binding of hydrophobic molecules to alkylated HA in the shell, poses difficulty in precisely controlling drug release.

Here, we describe a new kind of LbL-based hollow capsule based on hyaluronic acid−cyclodextrin conjugates that combine severable favorable features for use as a hydrophobic drug carrier, including CD inclusion complexation, the unique biological functions of hyaluronic acid, and the transport properties of the capsules. Using paclitaxel as a model anticancer drug, we show that these systems can selectively bind the anticancer drug in the shell and release it in a selective and controlled manner to breast cancer cells. To our knowledge, such capsules with cyclodextrin complexes incorporated in the multilayer shell remain scarcely investigated. A few studies previously demonstrated the ability to prepare capsules using the interaction between cyclodextrins and hydrophobic guest molecules (ferrocene, azobenzene, or adamantane) grafted to a polymer (poly(allylamine), poly(acrylic acid), or dextran) as the driving force in the LbL assembly.[12−14] The nanoshells showed responsiveness to environmental stimuli (pH variation and light irradiation). This property was exploited to control drug release by the destruction of the capsule. The originality here is to control drug release by the selective CD complexation in capsules that are recognizable by cancer cells and sensitive to enzymatic hydrolysis because of the unique biological properties of hyaluronic acid.

EXPERIMENTAL SECTION

Materials. The sample of bacterial sodium hyaluronate with a weight-average molecular weight of 200 kg/mol was supplied by ARD (Pomacle, France). The molecular weight distribution and the weight-average molecular weight were determined by size-exclusion chromatography using a Waters Alliance chromatograph equipped with two online detectors: a differential refractometer and a light-scattering detector (MALLS) from Wyatt. The solutions were injected at a concentration of 1 mg/mL in 0.1 M $NaNO_3$. The polydispersity index of the sample is M_w/M_n ∼1.5. 6-Monodeoxy-6-monoamino-β-cyclodextrin hydrochloride, heptakis-(2,6-di-*O*-methyl) β-CD (DM-β-CD), pentenoic anhydride, 3-mercaptopropionic acid (MPA), ethylenediaminetetraacetic acid (EDTA), phosphate buffered saline (PBS, pH 7.4), 1-ethyl-3-(3-dimethylaminopropyl) carbodiimide (EDC), *N*-hydroxysulfo-succinimide (sNHS), and all other chemicals were purchased from Sigma-Aldrich-Fluka and were used without further purification. Paclitaxel and Oregon Green-labeled paclitaxel (OG-PTX) were purchased from Invitrogen. 2-Hydroxy-1-[4-(2-hydroxyethoxy)phenyl]-2-methyl-1-propanone (Irgacure 2959) was kindly provided by Ciba Specialty Chemicals (Basel, Switzerland). Deuterium oxide was obtained from SDS (Vitry, France). The water used in all experiments was purified by a Elga Purelab purification system, with a resistivity of 18.2 MΩ cm. The β-cyclodextrin derivative monofunctionalized with MPA (CD-SH), used for the synthesis of CD-modified HA (HA-CD), was prepared in the laboratory as previously described.[15] The pentenoate-modified HA with a degree of substitution (DS; defined as the number of moles of CD molecules per 100 disaccharide repeating units) of nine was synthesized as previously described.[15]

Synthesis of HA-CD. To a solution of HA-pentenoate (80 mg, 1.57×10^{-2} mmol) in ultrapure water containing Irgacure 2959 (0.05% w/v) as a photoinitiator, CD-SH (20 mg, 1.57×10^{-2} mmol) dissolved in 1 mL of water was added. The grafting of CD-SH moieties was performed under UV irradiation (λ = 365 nm) for 10 min. The product was purified by diafiltration (ultramembrane Amicon YM10) with ultrapure water and was recovered by freeze-drying (95 mg). The degree of substitution of HA-CD was found to be 9 ± 1 by ^{1}H NMR (Figure SI 1).

^{1}H NMR (400 MHz, D_2O) δ (ppm): 4.95 (anomeric protons of CD), 4.55 (anomeric proton of the *N*-acetylglucosamine units), 4.25 (anomeric proton of the glucuronic acid units), 2.8−2.5 (2 CH_2CO, CH_2-S-CH_2), 1.85 (CH_3-CO from HA), 1.7−1.2 (2 CH_2)

Synthesis of (HA-CD/PLL) Capsules and Quantification of OG-PTX Incorporated in Capsules. Microcapsules were prepared according to the method described for the synthesis of (HA/PLL) capsules using calcium carbonate particles as a sacrificial template.[16] The $CaCO_3$ microparticles were synthesized from solutions of $CaCl_2$ and Na_2CO_3 as reported in the literature.[17] PTX was precomplexed with HA-CD by adding 34.2 μL of a PTX/OG-PTX mixture (5.85 mM) in methanol in the HA-CD solution (4 mL) at 1 g L^{-1}. The $CaCO_3$ particles were coated layer-by-layer by incubating them at a concentration of 2% (w/v) in solutions of HACD-PTX (at 1 g/L) and PLL (at 2 g/L), both in 0.15 M NaCl (pH 6.5). After the desired number of layers were deposited, the multilayer shell was cross-linked using EDC (400 mM) and sNHS (100 mM) in 0.15 M NaCl, and the $CaCO_3$ core was removed by treatment with an aqueous solution of EDTA (0.1 M, pH 7.2). The dissolved ions resulting from the decomposition of $CaCO_3$ were then removed by dialysis against pure water using spectra Por dialysis bags with a molecular weight cut off of 10 kDa.

The amount of OG-PTX incorporated in the capsules was determined by fluorescence intensity measurements after the extraction of PTX/OG-PTX from capsules with methanol according to an established procedure.[11] The suspension of capsules (100 μL at ∼6×10^7 capsules/mL) in PBS was centrifuged (4000 rpm, 4 min, 20 °C), and the supernatant was removed. After the addition of methanol, the suspension was again centrifuged (9000 rpm, 4 min, 20 °C), and the supernatant containing OG-PTX was recovered. This process was repeated two times to ensure the full extraction of OG-PTX from the capsules. Then, the solutions were analyzed using a fluorescence microplate reader (Infinite 1000, Tecan, Austria) with excitation and emission wavelengths set at 496 ± 10 and 524 ± 10 nm, respectively. To estimate the absolute OG-PTX concentration, a calibration curve for the fluorescence of OG-PTX as a function of its concentration was acquired (Figure SI 2). The effective concentration of PTX per capsule was calculated by knowing the ratio of unlabeled/labeled PTX, the molecular weight of PTX and OG-PTX, and the average number of

capsules per mL which was determined using a Petroff-Hausser counting chamber. The amount of PTX entrapped in the capsules was also analyzed by UV spectroscopy. The results obtained from this method confirmed those derived from the fluorescence intensity measurements.

Solubility Studies. Two PTX stock solutions were prepared in methanol (A, 1 g/L (1.17 mM) and B, 5 g/L (5.85 mM)). Solution A (1.7 μL) was added to an aqueous solution (1 mL) of β-CD ([CD] = 6 mM), and solution B (8.5 and 8.4 μL) was added to aqueous solutions (1 mL) of HA-CD ([CD] = 0.157 mM) and DM-β-CD ([CD] = 6 mM), respectively. The resulting mixtures were stirred gently for 4 h at room temperature, and methanol was allowed to evaporate slowly under a stream of nitrogen. The suspensions were then filtered through a 0.45 μm membrane filter (Millipore) and analyzed by UV spectrometry. The concentration of PTX in the solution was calculated using the Beer–Lambert law, $A = \varepsilon cl$, where A is the absorbance, c is the concentration in mol/L, l is the path length of the cell (l = 1.25 cm), and ε is the extinction coefficient (ε = 28 000).

Release Kinetics of Paclitaxel from (HA-CD/PLL) Capsules. The suspension of PTX-loaded capsules was divided in samples of 200 μL. Each sample was dispersed in 1.5 mL of PBS in an eppendorf tube at 37 °C. Periodically (two times per day), 1 mL of release medium was removed, and 1 mL of fresh PBS was added to each eppendorf tube. At time x, one sample was treated to determine the amount of PTX retained in the capsules. PTX was extracted from the capsules with methanol, and the methanolic solution was analyzed by UV spectrometry. This process was performed in duplicate.

Physicochemical Characterization. ^{1}H NMR spectra of CD and HA derivatives dissolved in deuterium oxide (6 mg/mL) were performed at 25 and 80 °C, respectively, using a Bruker spectrometer operating at 400 MHz.

The buildup of $(HA\text{-}CD/PLL)_i$, $(HA\text{-}CD\text{-}PTX/PLL)_i$, and $(HA/PLL)_i$ films (where i denotes the number of layer pairs) was followed by in situ quartz crystal microbalance with dissipation monitoring (QCM-D, D300, Qsense, Sweden) according to the experimental protocol that has been described in our previous publications.[18,19] For SEM observations, a drop of the capsules suspension is deposited on fresh clived mica and air dried. The samples were coated with a 2 nm layer of carbon and observed in the secondary electron imaging mode with a FEI Quanta 250 FEG-SEM using an accelerating voltage of 3 kV or sputtered with 8 nm layer of Au/Pd and observed in the secondary electron imaging mode with a Jeol JSM610 SEM using an accelerating voltage of 8 kV.

***In Vitro* Biocompatibility Studies. Cell Culture.** MDA-MB-231 cells were cultured in DMEM (Gibco, Invitrogen, USA) without pyruvate supplemented with 10% heat-inactivated fetal bovine serum (FBS, PAA Laboratories, France), 100 U/mL penicillin G, and 100 mg/mL streptomycin (Gibco, Invitrogen, USA) in a 37 °C, 5% CO_2 incubator. Cells were subcultured prior to reaching 60–70% confluence. For all experiments, MDA-MB-231 cells were seeded at 5000 cells per well in 96-well plates in 200 μL of medium and were allowed to grow for a total of 4 days. PTX in solution and unloaded and PTX-loaded microcapsules diluted to low (LD, 30 capsules/cell), medium (MD, 60 capsules/cell), or high density (HD, 120 capsules/cell) were added to the cells 24 h after cell plating.

Viability and Proliferation Assays. Cell viability was measured by a 3-(4,5-dimethylthiazol-2-yl)-2,5-diphenyltetrazolium bromide (MTT, Sigma) assay. At given time intervals, 25 μL of an MTT solution (1.5 mg/mL in PBS) was added to each well. The plates were then incubated for 75 min, allowing the viable cells to reduce the yellow MTT to dark-blue formazan crystals, which were subsequently dissolved in 200 μL of DMSO. The absorbance of the plate was measured using the microplate reader at 550 ± 5 nm and at 650 + 5 nm for the reference wavelength. Cell proliferation over time was quantified by counting the total number of cells in each well. Briefly, cells were detached with a 0.25% trypsin-EDTA solution for 5 min at 37 °C and then quantified using a Malassez chamber. Experiments were performed in triplicate, with three wells per condition in each experiment.

Immunostaining. Cells were fixed in 3.7% formaldehyde in PBS for 20 min and permeabilized for 4 min in TBS (0.15 M NaCl, 50 mM Tris-HCl, pH 7.4) containing 0.2% Triton X-100. The plates were blocked using TBS containing 0.1% BSA for 1 h and were then incubated with monoclonal antitubulin (Sigma) (1:200) antibodies in TBS with 0.2% gelatin for 30 min. AlexaFluor-643 goat antimouse IgG (Invitrogen) was then incubated for 30 min. Finally, nuclei were stained using Hoechst 33342 (Invitrogen) at 5 μg/mL for 10 min. The plates were viewed under confocal microscopy (LSM 700, Zeiss) using a 63× objective. Images were acquired with Zen 2010 software.

Statistical Analysis. All of the results are expressed as mean values ± standard error of the mean (SEM). Statistical comparisons were based on an analysis of variance (ANOVA) for pairwise comparisons ($p < 0.05$ was considered significant).

RESULTS AND DISCUSSION

To prepare capsules able to selectively entrap hydrophobic molecules within the nanoshell through host–guest complexation, HA modified by β-cyclodextrin was layer-by-layer assembled with poly(L-lysine) (PLL), a biocompatible and

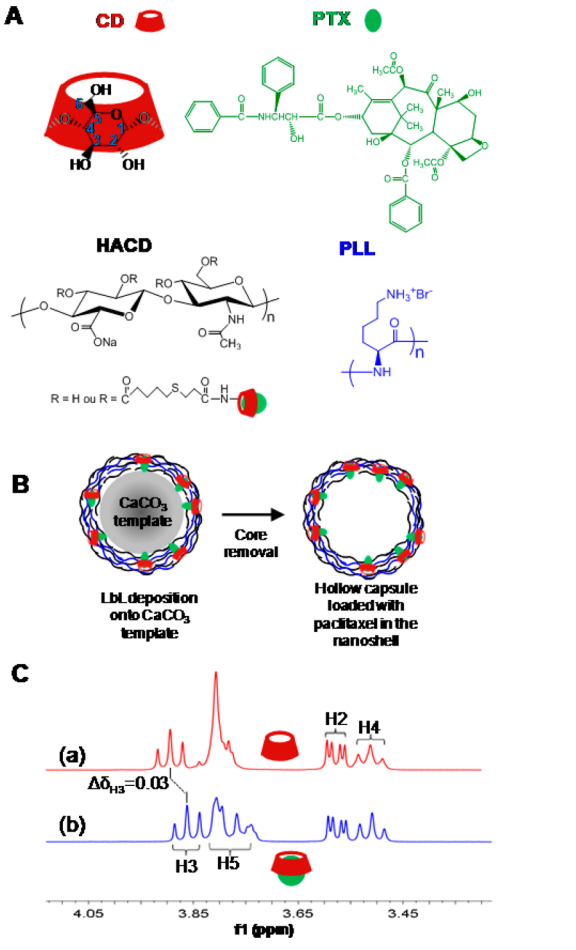

Figure 1. Strategy for the synthesis of capsules with host–guest complexes in the nanoshells. (A) Structures of β-CD, paclitaxel, and the biopolymers (HA-CD and PLL) forming the nanoshell. (B) Schematic representation of the fabrication of stable (HA-CD/PLL) capsules by cross-linking the (HA-CD/PLL) multilayer wall before dissolution of the calcium carbonate core templates. (C) Partial ^{1}H NMR spectra (400 MHz, 25 °C, D_2O) of (a) β-CD (10 mM) and (b) a mixture of β-CD (10 mM) and paclitaxel added at a concentration 2.5 μM.

dx.doi.org/10.1021/cm4019925 | Chem. Mater. 2013, 25, 3867–3873

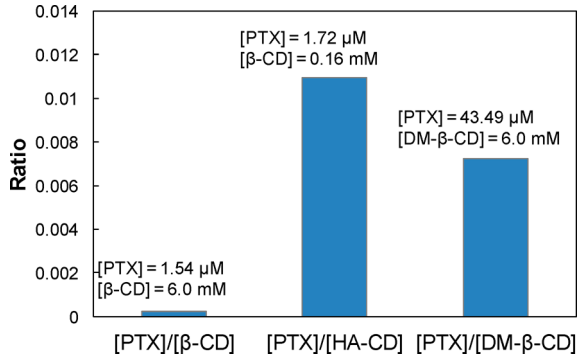

Figure 2. Complexation of PTX by HA-CD in aqueous solution: dependence of paclitaxel solubility in aqueous solutions containing natural β-CD, HA-CD, and DM-β-CD.

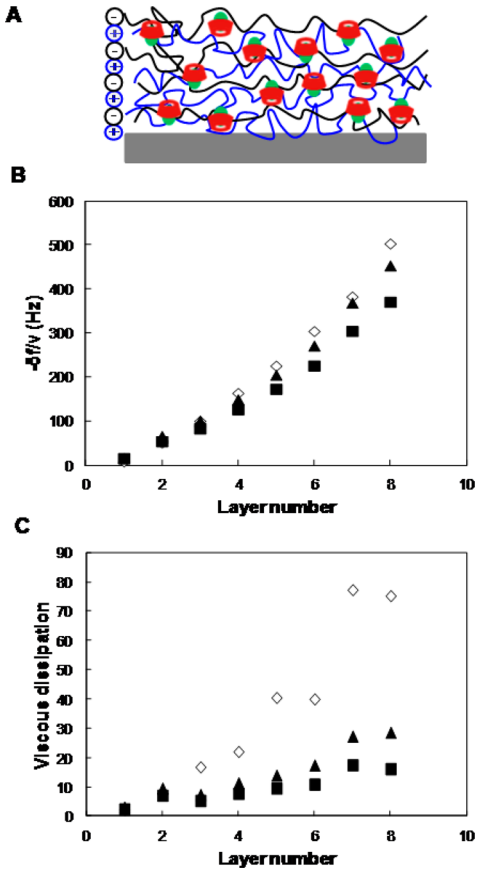

Figure 3. Growth of (HA-CD/PLL) films with and without PTX in 0.15 M NaCl (pH 6.5) measured by QCM-D on gold-coated crystal. (A) Schematic representation of a layer-by-layer self-assembled film of HA-CD/PLL. (B) Differences in the QCM frequency shifts measured at 15 MHz are plotted for each polyanion and PLL layer. Data are given at 15 MHz for HA-CD (■) and HA-CD-PTX (▲) as compared to unmodified HA (◊). (C) Viscous dissipations for each polyanion and PLL layer.

biodegradable polypeptide, on sacrificial colloidal particles (Figure 1A,B).

HA was selected as a polyanion because of its interesting biological properties. Indeed, HA is a natural glycosaminoglycan, which can be specifically recognized by the CD44 receptor that is overexpressed by several cancer cells.[20−23] For example, to develop breast cancer-targeted drug-delivery systems, HA has been previously reported as a targeting ligand for HA-

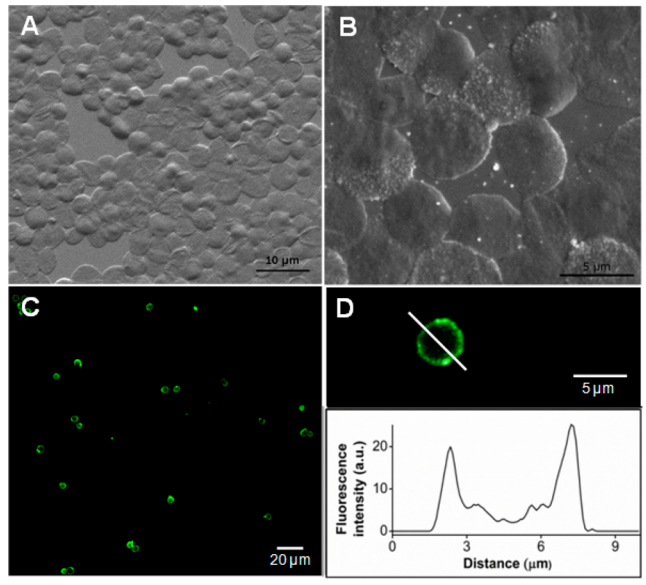

Figure 4. Microscopic observations of $((HA\text{-}CD\text{-}PTX)/PLL)_4/HA$ capsules. (A, B) SEM observations of the dried hollow capsules. (C) CLSM images of capsules exhibiting a localized green fluorescence in their nanoshell resulting from the complexation of OG-PTX by CD molecules in the nanoshell. (D) Magnified image of a capsule and the corresponding fluorescence intensity profile along its diameter, confirming the selectivity of OG-PTX incorporation in the nanoshell.

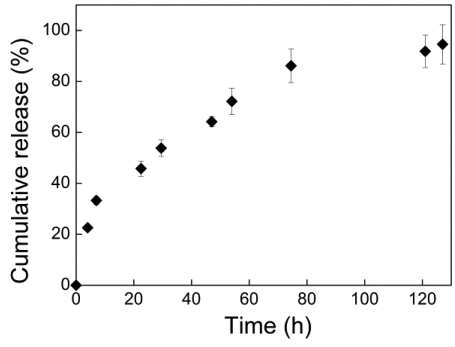

Figure 5. *In vitro* release profile of paclitaxel from the ((HA-CD-PTX)/PLL)4/HA capsules in PBS.

paclitaxel conjugates and[24] HA-grafted liposomes[23,25] as well as HA-coated poly(D,L-lactide-co-glycolide) nanoparticles.[26]

Moreover, we previously demonstrated that by using calcium carbonate particles and carefully optimizing the assembly conditions, stable nonaggregated (HA/PLL) capsules can be obtained after cross-linking of the (HA/PLL) film through EDC/sNHS-mediated amidation.[16]

HA was functionalized by β-cyclodextrin using a thiol-ene reaction. We recently reported the potential of this coupling strategy for the modular functionalization of polysaccharides.[15] The reaction consisted of the radical addition in aqueous solution of a β-cyclodextrin derivative monofunctionalized with mercaptopropionic acid onto pentenoate-modified HA. A quantitative coupling yield was obtained, leading to a HA-CD derivative with a DS of 9 from ^{1}H NMR analysis. ^{1}H NMR spectroscopy was also used to demonstrate the complexation of PTX by the natural β-CD cavity (Figure 1C). It is observed here that PTX induces large shifts in the NMR signals of the H-3 and H-5 protons located in the cavity, which is in contrast to the H-2 and H-4 protons located outside the cavity that clearly

dx.doi.org/10.1021/cm4019925 | *Chem. Mater.* 2013, 25, 3867−3873

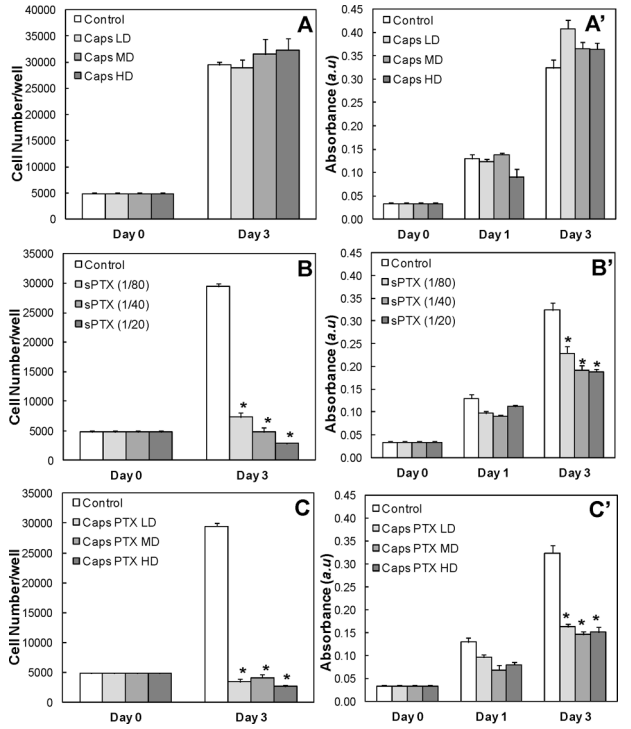

Figure 6. MDA-MB-231 cell response to unloaded microcapsules in solution, PTX in solution, and PTX-loaded $(HA\text{-}CD/PLL)_4/HA$ microcapsules. MDA-MB-231 cell number and MTT metabolic activity were quantified after 1 and 3 days in the presence of (A, A′) unloaded microcapsules added at increasing concentrations (LD, MD, or HD); (B, B′) with PTX added in solution to the cells at increasing concentrations (i.e., $^1/_{80}$ sPTX (0.0114 μM), $^1/_{40}$ sPTX (0.0228 μM), and $^1/_{20}$ sPTX (0.0457 μM) corresponding to LD, MD, and HD); and (C, C′) PTX-loaded microcapsules added at increasing densities (LD, MD, and HD) in the culture medium. Data represent the mean ± SEM of three wells. Experiments have been performed in triplicate. * $p < 0.05$.

demonstrate the formation of an inclusion complex. This allows for the improved solubility of paclitaxel in water.[27] In fact, PTX is characterized by a low solubility in water (0.4 μM or 0.34 μg/mL)[28] because of its high hydrophobicity. Therefore, PTX is difficult to administer and requires solubilization in a Cremophor EL (CrEL, a polyoxyethylated castor oil) and ethanol mixture (Taxol), which often lead to adverse side effects such as hypersensitivity reactions.[29] The enhancement of the water-solubility of PTX through host−guest interactions with the natural β-CD, HA-CD, and with the heptakis-(2,6-di-*O*-methyl) β-CD (DM-β-CD), which has a 30−fold higher aqueous solubility,[30] is shown in Figure 2.

In the case of the natural β-CD, the water-solubility of PTX is increased ∼5-fold for a PTX/β-CD molar ratio of 2.57×10^{-4} ([β-CD] = 6 mM), whereas in the case of HA-CD, the same increase is achieved for a PTX/β-CD molar ratio of 1.10×10^{-2} ([β-CD] = 0.16 mM). As the inclusion performances of the natural β-CD and grafted β-CD are of the same order of magnitude,[31] the extremely high-solubilization potential obtained with HA-CD is related to the high solubility in water of the host polysaccharide. As shown in Figure 2, a similar conclusion could be drawn comparing the solubilization power of the natural β-CD with that of DM-β-CD.

The assembly of HA-CD (with and without PTX) and PLL in multilayer films was confirmed by following (HA-CD/PLL) film deposition on a planar solid substrate by QCM-D (Figure 3). The film growth was found to be exponential and very similar to that of (PLL/HA).[16] The exponential growth could be related to the diffusion of PLL within the film architecture, as previously observed for (PLL/HA) films.[32]

We then investigated the generation of capsules made from (HA-CD/PLL) films and the PTX loading and release from the nanoshell. To this end, Oregon Green-labeled PTX (OG-PTX) was precomplexed with HA-CD, and the resulting HA-CD/PTX complex was assembled layer-by-layer with PLL on calcium carbonate microparticles. The spherical $CaCO_3$ particles, characterized by a quite narrow size distribution (diameter in the range 4−6 μm) and a positive surface charge under physiological conditions, were synthesized according to a previously described procedure.[17] After shell cross-linking by amide bond formation between HA and PLL and core dissolution by treatment with an aqueous solution of EDTA,[16] we successfully obtained hollow capsules. Observations of the OG-PTX-loaded capsules made of four (HA-CD/PLL) layer pairs and one HA layer in PBS solution by CLSM confirmed their spherical shape with a size of 4.2 ± 0.2 μm (measured on three different capsule batches) and green capsule shells (Figure 4).

Importantly, the intensity profile along a diameter confirmed the selective incorporation of OG-PTX in the shell as well as its impressive stability after core removal. Furthermore, fluorescence microscopy revealed that the drug-loaded capsules were well-dispersed in phosphate buffered saline. The SEM images also indicate diameters on the order of ∼5 μm for the dried capsules (Figure 4).

We quantified the amount of PTX entrapped in the capsules by fluorescence intensity measurements using OG-PTX. After extraction of PTX from the nanoshell with methanol,[11] the effective concentration of PTX in 100 μL of a capsule suspension at 6×10^7 capsules per mL was found to be 0.914 μM, corresponding to ∼13 fg of PTX per capsule. New batches of PTX-loaded capsules were then treated over time to examine the release of PTX under simulated physiological conditions (PBS, pH 7.4, 37 °C). As can be seen from Figure 5, PTX was released according to a two-step process with about 20% of the drug released in the first ∼4 h, after which there was a steady and controlled increase in release for up to 120 h. This sustained release profile, making PTX available within a period of 5 days, is attributed to the CD moieties that entrap the drug. Indeed, addition of DM-β-CD in the aqueous suspension of capsules triggered payload release with about 80% of PTX released in ∼20 h (Figure SI 3). The very small initial burst may be due to PTX encapsulated in the layers close to the surface. Indeed, a similar profile could be obtained under conditions limiting this potential phenomenon (i.e., by decreasing the [PTX]/[HA-CD] ratio during LbL film deposition). Taken together, these results highlight the ability of the multilayer shell to retain the vast majority of PTX within the capsule, which could potentially limit toxicity.

We then investigated the capacity of $(HA\text{-}CD/PLL)_4$-HA capsules to deliver PTX to MDA-MB-231 breast cancer cells, a cell line known to be sensitive to PTX.[33] After the extraction of PTX from the nanoshell, the effective concentration of PTX in 100 μL of a microcapsule suspension at 6×10^7 microcapsules/mL was found to be of 0.914 μM, corresponding to ∼13 fg of PTX per microcapsule. This value was taken as the positive reference for tests using PTX in solution (= sPTX). Unloaded and PTX-loaded capsules at different densities were added to

dx.doi.org/10.1021/cm4019925 | *Chem. Mater.* 2013, 25, 3867−3873

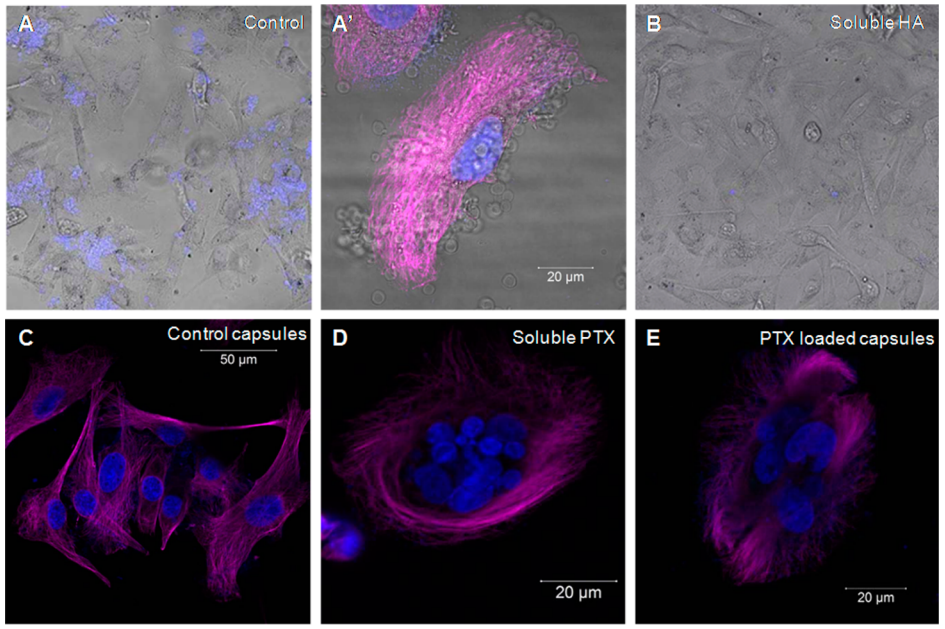

Figure 7. Microscopic observations of capsule/MDA-MB-231 cell interactions after 24 h of culture. (A, A′) Interaction of HA-containing capsules with MDA-MB-231 cells (nuclei stained in blue and β-tubulin in pink). (B) Interaction is inhibited by adding soluble HA to the culture medium. (C−E) Immunostaining of β-tubulin (pink) and nuclei (blue) in representative MDA-MB-231 cells after 24 h of culture (C) in contact with control capsules at HD (120 capsules/cell), (D) in contact with soluble PTX at 0.0228 μM ($^1/_{40}$), and (E) in contact with PTX-loaded capsules at MD (60 capsules/cell).

MDA-MB-231 cells in culture and observed over 3 days. The cytotoxicity of the capsules was evaluated by counting the cell number and by measuring cell viability using an MTT assay.[11] Unloaded microcapsules added at increasing concentrations to the cells did not induce any cytotoxic effect, even when added at a high density (HD, ∼120 caps./cell) to the cell culture (Figures 6A,A′ and SI4). The addition of PTX in solution (Figure 6B,B′) led to a significant decrease of cell number and cell metabolic activity, as anticipated.

Notably, the PTX-loaded capsules exhibited an important effect on MDA-MB-231 cells (Figure 6C,C′), strongly limiting their proliferation and metabolic activity. At day 3, the number of cells cultivated in the presence of the PTX-loaded capsules was between 7.2- to 8.6-fold lower than the cells cultivated in the absence of capsules or in the presence of unloaded capsules. Moreover, PTX-loaded capsules showed a higher effective cytotoxicity to MDA-MB-231 cells than that of PTX in solution (Figure SI 5). This effect was more significant in the case when lower PTX concentrations were used. This was probably due to the accumulation of capsules around MDA-MB-231 cells, leading to a local increase of PTX concentration. MDA-MB-231 cells are known to express CD44,[21,24] one of the hyaluronan receptors. Indeed, we verified that CD44 is highly expressed by the cancer cells (Figure SI 6).

In the presence of $(HA\text{-}CD/PLL)_4/HA$ capsules, we noted that several capsules interacted with the MDA-MB-231 cells (Figure 7A,A′). The OG-PTX-loaded capsules were in close contact with the cells, but no internalization of the capsules could be observed (Figure SI 7). This is in line with previous experiments showing that these cancer cells are unable to internalize capsules of ∼4 μm in diameter.[34]

Of note, when soluble HA was added to the culture medium, the interaction was fully inhibited (Figure 7B). Thus, the interaction of the HA-containing capsules and the cancer cells appears to be specifically mediated by the CD44 receptor.

MDA-MB-231 cells are also known to secrete hyaluronidase, an enzyme that can specifically degrade hyaluronan[35] and is overexpressed in malignant breast cancer cells.[36] Hyaluronidase is often used as a marker for tumor detection.[37] It may also well be that the cells locally degrade the HA-containing microcapsules.

Next, we investigated the effect of PTX on cell internal organization. Indeed, PTX is known to drastically affect cell internal structures, especially nuclear and microtubule organization.[38] We thus examined by immunostaining the organization of β-tubulin and the nucleus (Figure 7C−E). On control cells (no capsules or unloaded capsules), the nuclei were intact and the microtubule network was well organized (Figures 7C and data not shown). When PTX was added in the solution, bundles of microtubules were visible, and the nuclei were fragmented (Figure 7D). In the presence of PTX-loaded capsules, the fragmentation of the nuclei was particularly visible at high density, and bundles of microtubules were also visible after 1 day of culture (Figure 7E). This stabilization of the microtubules resulted in defects in cell mitosis and the presence of large, multinucleated cells. As a consequence, these deficiencies in cell division lead to a very low cell proliferation, as shown by the proliferation assay (Figure 6).

All together, our data suggest that the mechanism of action of the PTX-loaded capsules is based on the combined action of several phenomena: specific interactions with MDA-MB-231 cancer cells via the CD44 receptor, passive transfer of PTX from the CD cavities to the hydrophobic lipid membrane of the cells, and local degradation of the capsules by hyaluronidase enzyme secreted by these cells.

■ CONCLUSIONS

We designed and prepared under mild physiological conditions a new kind of LbL capsules containing the hydrophobic anticancer drug paclitaxel in the shell. The synthesis of these

dx.doi.org/10.1021/cm4019925 | Chem. Mater. 2013, 25, 3867−3873

capsules relied on the very high affinity of PTX to hyaluronic acid grafted with β-CD through inclusion complexation as well as on the ability of HA-CD-PTX to be layer-by-layer assembled with poly(L-lysine) on sacrificial colloidal particles. These capsules, combining the inclusion capacity of β-CD and the unique biological properties of HA, exhibited controlled release properties and were effective at killing breast cancer cells. Importantly, the cell viability and proliferation data demonstrated the enhanced potency of the encapsulated drug, suggesting that PTX is directly and continuously released from the capsules to the cancer cells. These results seem to be related to HA, which can specifically interact with the cancer cells overexpressing the CD44 receptor and be degraded by the hyaluronidase enzyme secreted by these cells. All together, these results indicate that these HA-CD-based capsules have the potential for use in the controlled delivery of hydrophobic drugs to cancer cells.

■ ASSOCIATED CONTENT

Supporting Information

^{1}H NMR spectrum of HA-CD, calibration curve of PTX, release profile in the presence of a competitive host molecule, images of cells incubated with capsules, comparison of cell response to PTX-loaded microcapsules and to PTX in solution, image of cancer cells stained for the hyaluronic acid receptor, and image of OG-PTX-loaded capsules/MDA-MB-231 cell interaction (PDF). This material is available free of charge via the Internet at http://pubs.acs.org.

■ AUTHOR INFORMATION

Corresponding Author

*E-mail: rachel.auzely@cermav.cnrs.fr.

Notes

The authors declare no competing financial interest.

■ ACKNOWLEDGMENTS

The authors gratefully acknowledge the financial support provided by the Agence Nationale pour la Recherche (grant ANR-07-NANO-002 to R.A.V. and C.P.) and by the European Commission (FP7 program) via a European Research Council starting grant (BIOMIM, GA 259370 to C.P.). R.A.V. and C.P. are indebted to the Institut Universitaire de France for financial support.

■ REFERENCES

(1) Agarwal, A.; Lvov, Y.; Sawant, R.; Torchilin, V. *J. Controlled Release* **2008**, *128*, 255−260.

(2) Smith, R. C.; Riollano, M.; Leung, A.; Hammond, P. T. *Angew. Chem., Int. Ed.* **2009**, *48*, 8974−8977.

(3) Wang, Y.; Yan, Y.; Cui, J.; Hosta-Rigau, L.; Heath, J. K.; Nice, E. C.; Caruso, F. *Adv. Mater.* **2010**, *22*, 4293−4297.

(4) Duncan, R. *Adv. Drug Delivery Rev.* **2009**, *61*, 1131−1148.

(5) Farokhzad, O. C.; Langer, R. *ACS Nano* **2009**, *3*, 16−20.

(6) Loomis, K.; McNeeley, K.; Bellamkonda, R. V. *Soft Matter* **2011**, *7*, 839−856.

(7) Uekama, K.; Hirayama, F.; Irie, T. *Chem. Rev.* **1998**, *98*, 2045−2076.

(8) Devi, N. K. D.; Rani, A. P.; Javed, M. M.; Kumar, K. S.; Kaushik, J.; Sowjanya, V. *Pharmacophore* **2010**, *1*, 155−165.

(9) Hayashi, K.; Ono, K.; Suzuki, H.; Sawada, M.; Moriya, M.; Sakamoto, W.; Yogo, T. *ACS Appl. Mater. Interfaces* **2010**, *2*, 1903−1911.

(10) Yan, Y.; Ochs Christopher, J.; Such Georgina, K.; Heath Joan, K.; Nice Edouard, C.; Caruso, F. *Adv. Mater.* **2010**, *22*, 5398−403.

(11) Cui, D.; Jing, J.; Boudou, T.; Pignot-Paintrand, I.; De Koker, S.; De Geest, B. G.; Picart, C.; Auzély-Velty, R. *Adv. Mater.* **2011**, *23*, H200−H204.

(12) Luo, G.-F.; Xu, X.-D.; Zhang, J.; Yang, J.; Gong, Y.-H.; Lei, Q.; Jia, H.-Z.; Li, C.; Zhuo, R.-X.; Zhang, X.-Z. *ACS Appl. Mater. Interfaces* **2012**, *4*, 5317−5324.

(13) Xiao, W.; Chen, W.-H.; Zhang, J.; Li, C.; Zhuo, R.-X.; Zhang, X.-Z. *J. Phys. Chem. B* **2011**, *115*, 13796−13802.

(14) Wang, Z.; Feng, Z.; Gao, C. *Chem. Mater.* **2008**, *20*, 4194−4199.

(15) Mergy, J.; Fournier, A.; Hachet, E.; Auzély-Velty, R. *J. Polym. Sci., Part A: Polym. Chem.* **2012**, *50*, 4019−4028.

(16) Szarpak, A.; Cui, D.; Dubreuil, F.; De Geest, B. G.; De Cock, L. J.; Picart, C.; Auzély-Velty, R. *Biomacromolecules* **2010**, *11*, 713−720.

(17) Volodkin, D. V.; Larionova, N. I.; Sukhorukov, G. B. *Biomacromolecules* **2004**, *5*, 1962−1972.

(18) Richert, L.; Lavalle, P.; Payan, E.; Shu, X. Z.; Prestwich, G. D.; Stoltz, J.-F.; Schaaf, P.; Voegel, J.-C.; Picart, C. *Langmuir* **2004**, *20*, 448−458.

(19) Schneider, A.; Vodouhe, C.; Richert, L.; Francius, G.; Le Guen, E.; Schaaf, P.; Voegel, J.-C.; Frisch, B.; Picart, C. *Biomacromolecules* **2007**, *8*, 139−145.

(20) Auzenne, E.; Ghosh, S. C.; Khodadadian, M.; Rivera, B.; Farquhar, D.; Price, R. E.; Ravoori, M.; Kundra, V.; Freedman, R. S.; Klostergaard, J. *Neoplasia* **2007**, *9*, 479−486.

(21) Draffin, J. E.; McFarlane, S.; Hill, A.; Johnston, P. G.; Waugh, D. J. J. *Cancer Res.* **2004**, *64*, 5702−5711.

(22) Luo, Y.; Prestwich, G. D. *Bioconjugate Chem.* **1999**, *10*, 755−763.

(23) Qhattal, H. S. S.; Liu, X. *Mol. Pharmaceutics* **2011**, *8*, 1233−1246.

(24) Luo, Y.; Ziebell, M. R.; Prestwich, G. D. *Biomacromolecules* **2000**, *1*, 208−218.

(25) Surace, C.; Arpicco, S.; Dufay-Wojcicki, A.; Marsaud, V.; Bouclier, C.; Clay, D.; Cattel, L.; Renoir, J.-M.; Fattal, E. *Mol. Pharmaceutics* **2009**, *6*, 1062−1073.

(26) Hyung, W.; Ko, H.; Park, J.; Lim, E.; Park, S. B.; Park, Y.-J.; Yoon, H. G.; Suh, J. S.; Haam, S.; Huh, Y.-M. *Biotechnol. Bioeng.* **2007**, *99*, 442−454.

(27) Hamada, H.; Ishihara, K.; Masuoka, N.; Mikuni, K.; Nakajima, N. *J. Biosci. Bioeng.* **2006**, *102*, 369−371.

(28) Sharma, U. S.; Balasubramanian, S. V.; Straubinger, R. M. *J. Pharm. Sci.* **1995**, *84*, 1223−30.

(29) Gelderblom, H.; Verweij, J.; Nooter, K.; Sparreboom, A. *Eur. J. Cancer* **2001**, *37*, 1590−1598.

(30) Auzély-Velty, R.; Djedaïni-Pilard, F.; Desert, S.; Perly, B.; Zemb, T. *Langmuir* **2000**, *16*, 3727−3734.

(31) Charlot, A.; Heyraud, A.; Guenot, P.; Rinaudo, M.; Auzély-Velty, R. *Biomacromolecules* **2006**, *7*, 907−913.

(32) Picart, C.; Mutterer, J.; Richert, L.; Luo, Y.; Prestwich, G. D.; Schaaf, P.; Voegel, J. C.; Lavalle, P. *Proc. Natl. Acad. Sci. U.S.A.* **2002**, *99*, 12531−12535.

(33) Frasci, G.; Comella, P.; D'Aiuto, G.; Budillon, A.; Barbarulo, D.; Thomas, R.; Capasso, I.; Casaretti, R.; Daponte, A.; Caponigro, F.; Gravina, A.; Maiorino, L.; Carateni, G.; Gentile, A.; Comella, G. *Breast Cancer Res. Treat.* **1998**, *49*, 13−26.

(34) Boudou, T.; Kharkar, P.; Jing, J.; Guillot, R.; Pignot-Paintrand, I.; Auzély-Velty, R.; Picart, C. *J. Controlled Release* **2012**, *159*, 403−412.

(35) Menzel, E. J.; Farr, C. *Cancer Lett.* **1998**, *131*, 3−11.

(36) Tan, J.-X.; Wang, X.-Y.; Li, H.-Y.; Su, X.-L.; Wang, L.; Ran, L.; Zheng, K.; Ren, G.-S. *Int. J. Cancer* **2010**, *128*, 1303−1315.

(37) Li, Y.; Li, L.; Brown, T. J.; Heldin, P. *Int. J. Cancer* **2007**, *120*, 2557−2567.

(38) Yeung, T. K.; Germond, C.; Chen, X.; Wang, Z. *Biochem. Biophys. Res. Commun.* **1999**, *263*, 398−404.